**Table 3. Dynamic material properties of layers**

| Materials | Shear Wave Velocity (m/sec) | Shear Modulus (MPa) | Poisson's Ratio | Unit Weight ($g/cm^3$) |
|---|---|---|---|---|
| Uncontrolled fill | 200 | 76.6 | 0.35 | 1.92 |
| Marine clay | 90 to 120 | 14.4 to 23.9 | 0.45 | 1.60 |
| Glacial soil | 245 | 119.7 | 0.35 | 1.92 |

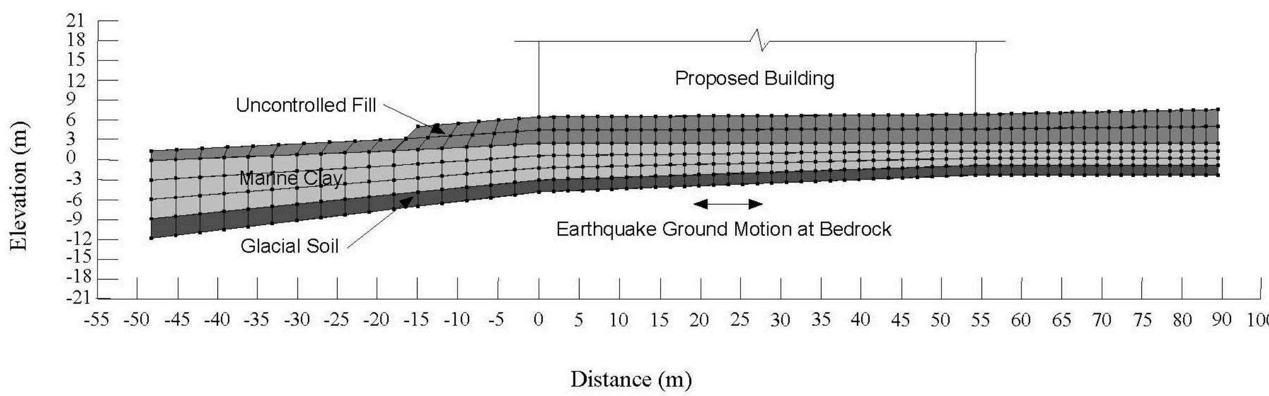


**Figure 4. Finite element model of east-west section**

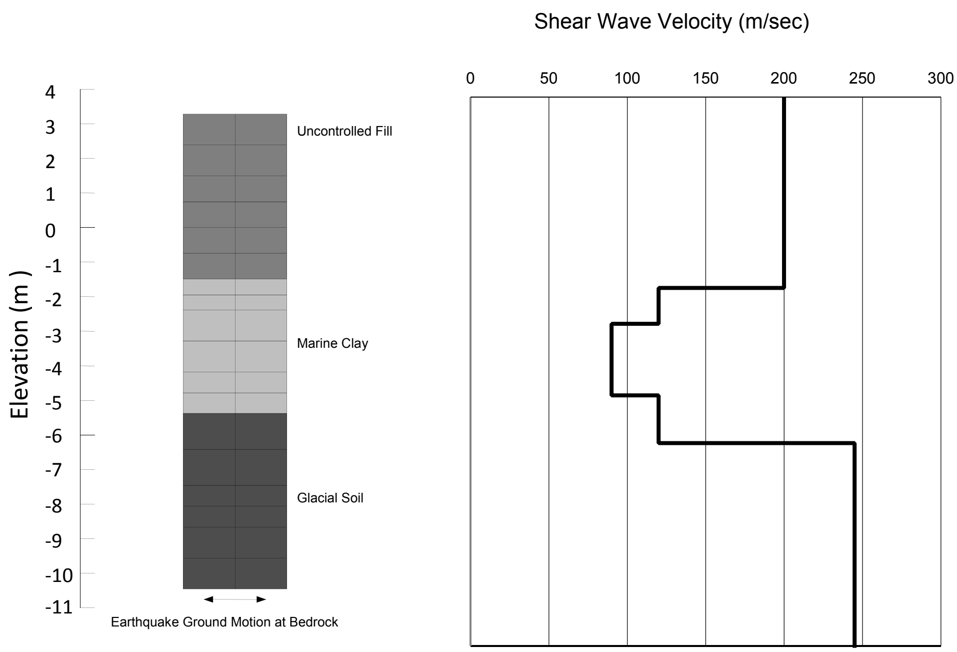


**Figure 5. Finite element model of single column with shear wave velocity profile**

As shown in Figs. 4 and 5, two-dimensional quadrilateral elements were used to model the soil. The shear wave velocity value for each layer as listed in Table 3 are plotted with depth along the single column model in Figure 5. For both 1-D and 2-D FEM models, the bottom boundary is assumed to be a fixity at bedrock and the side boundaries are restrained in the vertical direction and free to move horizontally. The five selected earthquakes are modified to meet the specified levels as ground motion inputs (in the form of acceleration time history) at the bedrock boundary. Time history analysis is performed at an interval of 0.02 sec throughout the input duration varying between 20 and 40 sec to develop responses at the ground surface.

## ANALYSIS FINDINGS

Finite element analysis results in the forms of ground surface spectral response acceleration are presented in Figs. 6 to 10. The amplifications represented by the site coefficients $F_a$ and $F_v$ are generated through comparing the spectral input at bedrock to those at the ground surface in accordance with IBC (2009) and plotted in Figs. 11 to 15. The weighted averages of spectral acceleration around 0.2 sec period (from 0 to 0.4 sec) and 1.0 sec period (from 0.5 to 1.5 sec) are used for calculating the amplifications. The methodology and justifications for the averaging are discussed by Borcherdt (1994). The findings are summarized as follows:

1. The site coefficient $F_a$ for the short-period surface spectral acceleration using the single column analysis varies between 0.76 and 0.94 for the five earthquake records. The magnitude of the acceleration spectrum within the short period band (between 0 and 0.5 sec) is subsided. As shown, the peak acceleration has shifted to the right in all cases (Figs. 6 to 10) as result of the earthquake transmitting through the soil media, with its
2. magnitude either increased or decreased. In contrast, the response spectrum from the sloping soil/rock profile is substantially amplified. The average amplification is about 1.5 for all five earthquakes. Variation of $F_a$ is not substantial along the horizontal profile (as the depth to rock varies).
3. The site coefficient $F_v$ of the 1-sec period surface spectral acceleration typically increases with thickness of the soil profile. However, this trend does not hold near the ends of the sloping soil/rock profile. On the far left end, where the soil is thickest, $F_v$ either increases or decreases without a pattern. These phenomena appear to be attributed to the drop of ground elevation. On the far right, the behavior of $F_v$ is similar to that on the far left but its change is minor.
4. The single soil column analyses yield a somehow similar coefficient of $F_v$ corresponding to the left end of the sloping soil/rock profile (east-west section) which is represented more or less by the single column in terms of overburden thickness.
5. $F_a$ and $F_v$ are developed by averaging the spectrum over a band of period. For $F_a$, the band range can be from 0 to 0.4 sec or from 0 to 0.5 sec. The results of $F_a$ usually do not vary greatly with the band width. However, $F_v$ varies substantially depending on the band range. Typically, a narrower band, e.g., 0.5 to 1.5 sec yields a higher average of $F_v$ than a wider band, e.g., 0.4 to 2.0 sec.

## CONCLUSIONS

Short period responses across a sloping rock are substantially magnified in the 2-D analysis. The single soil column 1-D analysis underestimates the short period response and thus the site coefficient $F_a$, compared to the 2-D analysis. The site coefficient $F_v$ of the 1-sec period surface acceleration spectrum typically increases with thicker soil profile.

1-D *SHAKE* analysis or single soil column (finite element) analysis can be used for generally horizontal soil and rock profile. When site conditions indicate a sloping soil/rock profile or highly variable depth to rock, the result from a 1-D analysis is questionable and the analysis may not be conservative for short period responses. Therefore, 2-D finite element analysis should be used to capture the variations in the soil/rock profile.

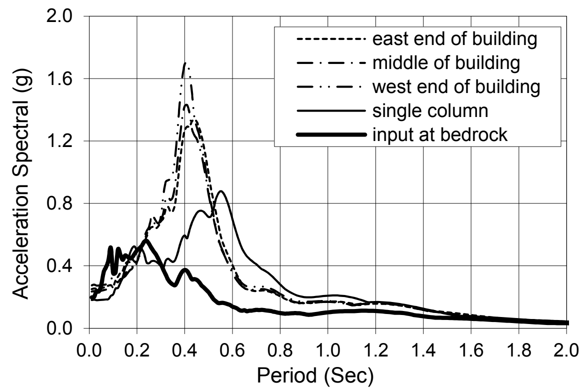


**Figure 6. Response spectral acceleration from modified El Centro 1940**

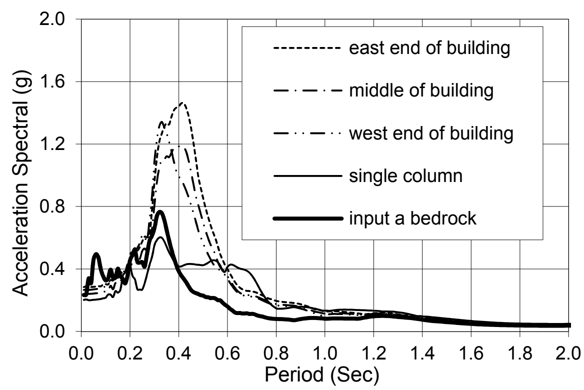


**Figure 7. Response spectral acceleration from modified Loma Prieta 1989**

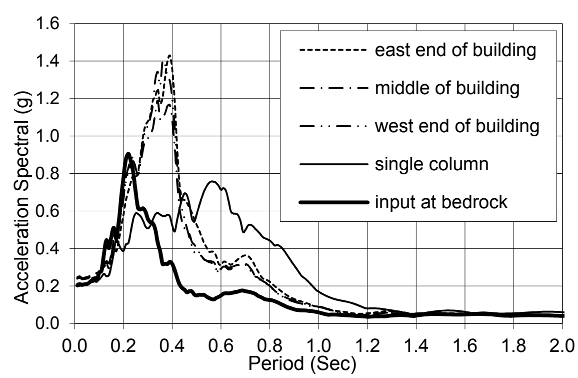


**Figure 8. Response spectral acceleration from modified Northridge 1994**

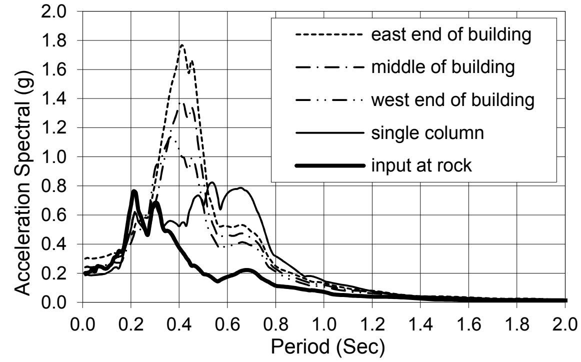


**Figure 9. Response spectral acceleration from modified NY Massena 1944**

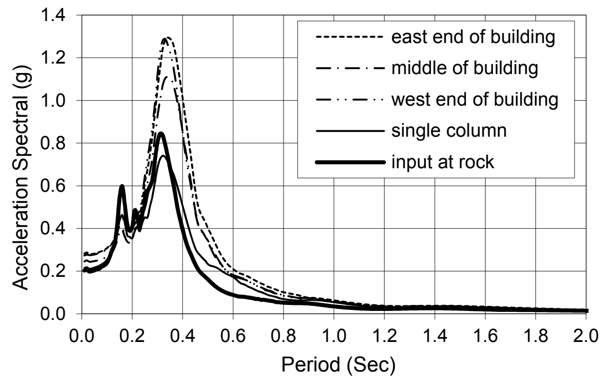


**Figure 10. Response acceleration spectral from modified NH Franklin Falls Dam 1982**

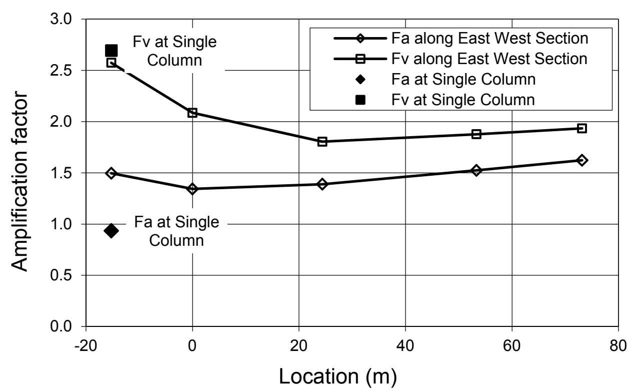


**Figure 11. Site coefficients $F_a$ and $F_v$ from modified El Centro 1940**

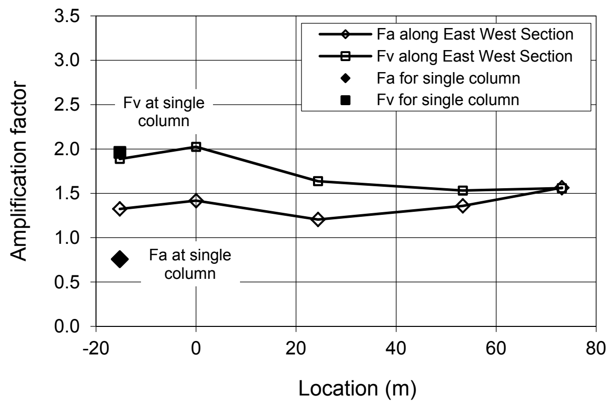


**Figure 12. Site coefficients $F_a$ and $F_v$ from modified Loma Prieta 1989**

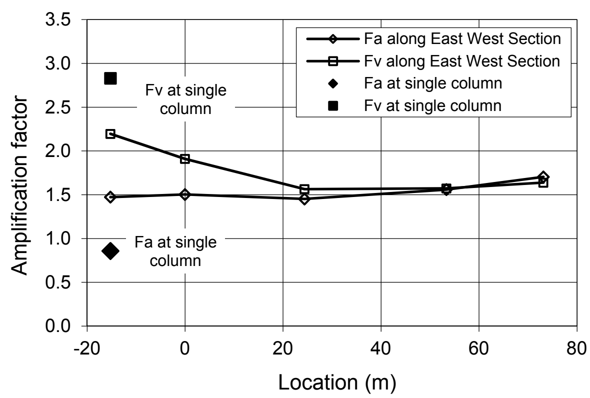


**Figure 13. Site coefficients $F_a$ and $F_v$ from modified Northridge 1994**

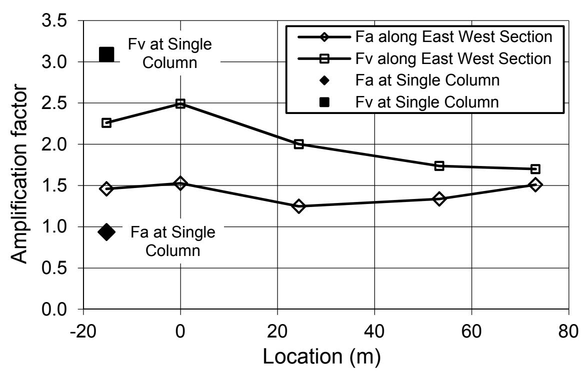


**Figure 14. Site coefficients $F_a$ and $F_v$ from modified NY Massena 1944**

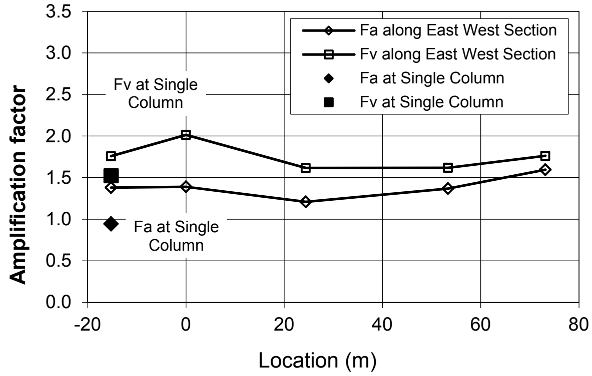


**Figure 15. Site coefficients $F_a$ and $F_v$ from modified NH Franklin Falls Dam 1982**

## REFERENCES


Bocherdt, R. D. (1994). "Estimates of Site-Dependent Response Spectra for Design (Methodology and Justification)." *Earthquake Spectra*, Vol. 10, No. 4, US Geological Survey.

Campanella, R. G., Robertson, P. K., and Gillespie, D. (1986). "Seismic cone penetration tests." *Use of In-Situ Tests in Geotechnical Engineering*, GSP 6, ASCE, Reston, VA, pp. 116-130.

Von Hake, C. A. (1975). *Earthquake Information Bulletin*, Volume 7, Number 4.

Crone, A. J. and Wheeler, R. L. (2002). *Data for Quaternary Faults, Liquefaction Features, and Possible Tectonic Features in the Central and Eastern United States, East of the Rocky Mountain Front*, Open-File Report 00-260, U.S. Department of the Interior, U.S. Geological Survey.

Frankel, A. D., Petersen, M. D., Mueller, C. S., Haller, K. M., Wheeler, R. L., Leyendecker, E. V., Wesson, R. L., Harmsen, S. C., Cramer, C. H., Perkins, D. M., and Rukstales, K. S. (2002). *Documentation for the 2002 Update of the National Seismic Hazard Maps,* Open-File Report 02-240, USGS.

Frankel, A. D., Mueller, C. S., Barnhard, T., Perkins, D. M., Leyendecker, E. V., Dickman, N., Harmsen, S. C., and Hopper, M. (1996). *National Seismic-Hazard Maps: Documentation*, Open-File Report 96-532, USGS.

Frankel, A. D. (1995). "Mapping Seismic Hazard in the Central and Eastern United States," *Seism. Res. Letts*, Vol. 66, No. 4, pp. 8-21.

Krahn, J. (2004). *Dynamic Modeling with QUAKE/W*, 1st Ed. Geo-Slope International, Ltd. Calgary Alberta, Canada.

http://earthquake.usgs.gov/research/hazmaps/products_data/2002/ceus2002.php

Idriss, I. M. and Sun, J. I. (1992). *User's Manual for SHAKE91, A Computer Program for Conducting Equivalent Linear Seismic Response Analysis of Horizontally Layered Soil Deposits.* Center for Geotechnical Modeling, Dept. of Civil & Environmental Engineering, University of California, Davis.

IBC (2009). *2009 Internation Building Code (IBC)*, International Code Council.

Ishibashi, I. and Zhang, X. (1993). "Unified Dynamic Shear Moduli and Damping Ratios of Sand and Clay." *Soils and Foundations*, Vol. 33, No. 1, pp. 182-191.

Schnabel, P. B, Lysmer, J., and Seed, H. B. (1972). *SHAKE: A Computer Program for Earthquake Response Analysis of Horizontally Layered Sites*. Report No. EERC 72-12, University of California, Berkeley, Dec., 102p.

Stover, C. W. and Coffman, J. L. (1993). *Seismicity of the United States, 1568-1989 (Revised)*, U.S. Geological Survey Professional Paper 1527, United States Government Printing Office, Washington DC.

# Weathered Zone Effects: Central and Eastern North American Site Response

**Morgan A. Eddy, P.E., M.Sc.[1]; C. Guney Olgun, Ph.D.[2]; Adrian Rodriguez-Marek, Ph.D.[3]; and Martin C. Chapman, Ph.D.[4]**

[1]Steele Foundation, LLC, 3299 K St. NW #601, Washington, DC 20007.
E-mail: morgan@steelefoundationllc.com
[2]Via Dept. of Civil and Environmental Engineering, Virginia Tech, 111A Patton Hall, Blacksburg, VA 24061. E-mail: olgun@vt.edu
[3]Via Dept. of Civil and Environmental Engineering, Virginia Tech, 214 Patton Hall, Blacksburg, VA 24061. E-mail: adrianrm@vt.edu
[4]Dept. of Geosciences, Virginia Tech, 4044 Derring Hall, Blacksburg, VA 24061.
E-mail: mcc@vt.edu

**Abstract**

This study quantifies uncertainty in Central and Eastern North America (CENA) Reference Rock (RR), Weathered Zone (WZ), and resulting earthquake ground surface site response predictions. The assumptions used for modeling the WZ have an effect on the predicted ground surface response. Random modeling of the RR and WZ is implemented using a simple Taylor Series expansion. Equivalent linear site response analysis is performed with a synthetically generated motion and includes the site attenuation parameter, kappa (κ), for modeling site damping. Probabilistic site response spectra and ratios of response spectra are presented. This study introduces a simple method for quantifying uncertainty in ground surface response while capturing RR and WZ variability.

## BACKGROUND

Weathering of rock can vary significantly over short distances leading to a variable rock surface and thickness/strength of residual materials above intact rock. This can have significant impacts on the response of a site during an earthquake. For example, Lester and Chapman (2005) present analyses performed at sites near Columbia, SC showing that the weathered zone tends to amplify ground surface site response.

The objective of this study is to develop a probabilistic site amplification model of Central and Eastern North America (CENA) accounting for uncertainties in reference rock and the weathered zone. The fundamental relationships between reference rock and the weathered zone are first presented in a base model. The base model is then modified to incorporate parameter uncertainties within a probabilistic framework.

## BASE MODEL

A simple base model of the CENA reference rock and weathered zone is subsequently presented. The base model consists of three layers: (1) the hard rock halfspace (HRH), (2) the reference rock (RR), and (3) the weathered zone (WZ). Figure 1 provides a schematic illustrating the three model layers. The HRH layer has a shear wave velocity of 3,500 m/s, $V_{s\text{-}HRH}$. The most likely shear wave velocity at the top of the RR layer, $V_{s\text{-}tRR}$ is 3,000 m/s and the layer is modeled with a unit weight of 27 kN/m$^3$ (after Hashash et al., 2014). The most likely shear wave velocity at the top of the WZ layer, $V_{s\text{-}tWZ}$ is 2,000 m/s after Hashash et al (2014). The thicknesses of the RR and WZ layers are referred to as $H_{RR}$ and $H_{WZ}$, respectively.

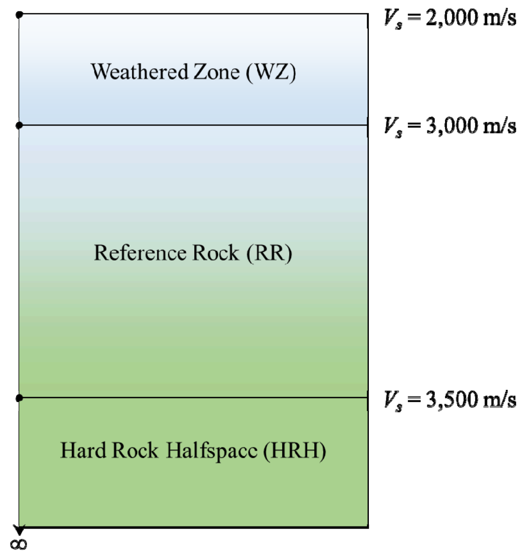


**Figure 1. Schematic of reference rock and weathered zone velocity model (not to scale).**

Site attenuation is incorporated into the base model with the site attenuation parameter, $\kappa_o$ after Anderson and Hough (1984). The $\kappa_o$ parameter is computed with Equation 1:

$$\kappa_o = \sum \frac{H_i}{V_{si} Q_i} \qquad \text{Eq. (1)}$$

Where $H_i$ is layer thickness, $V_{si}$ is the shear wave velocity of the layer and $Q_i$ is the dimensionless quality factor; all for the $i^{th}$ layer. Kappa is not directly related to the total thickness, average $Vs$ and Q but rather the integration of these parameters over the entire layer thickness. The kappa for each individual model layer, $\kappa_{RR}$ and $\kappa_{WZ}$, the kappa for each is computed by summing over the respective model sublayer thicknesses. For the purpose of simplifying the base model, $\kappa_o$ estimates are assumed to be discrete.

The quality factor is a function of shear wave velocity and is computed with Equation 2:

$$Q = \gamma V_s \qquad \text{Eq. (2)}$$

Where $\gamma$ is the linear quality-velocity ratio; similar to kappa, the quality factors are computed for each sublayer ($i$). The small-strain damping ratio in decimal format, $\zeta$, can then be computed with Equation 3.

$$\zeta_i = \frac{1}{2Q_i} \qquad \text{Eq. (3)}$$

Campbell (2009) presents relationships between $V_s$ and $Q$ for semi-consolidated sediments in Eastern North America shown in Figure 2. Campbell's plot indicates that $Q$ values and the corresponding quality-velocity ratios contain uncertainty. The uncertainty can be a combination of model or computational errors, the actual distributions and spatial variability of the parameters in the field.

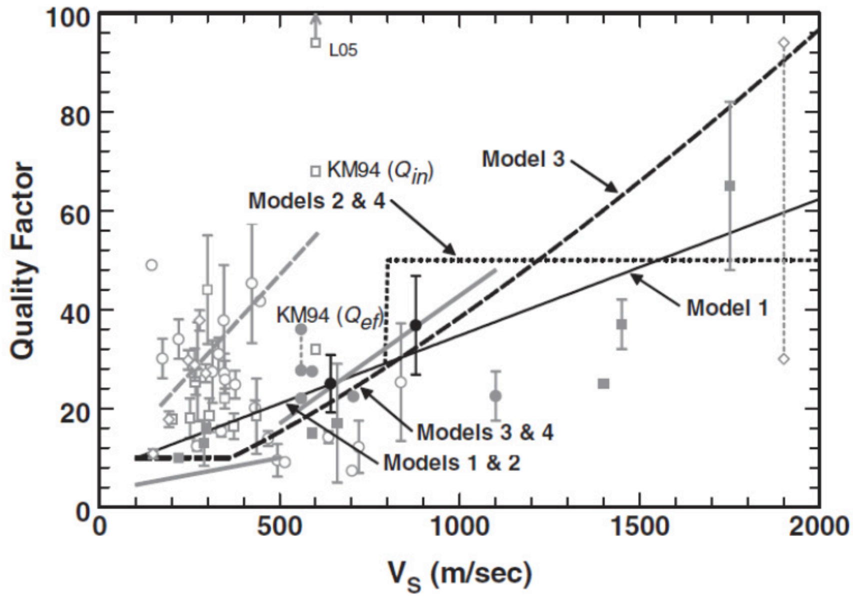


**Figure 2. $Q$ versus $V_s$ (from Campbell, 2009) from studies of Eastern North American semi-consolidated sediments.**

Hashash et al. (2014) recommend that the site attenuation parameter for the RR layer, $\kappa_{RR}$, ranges from 0.002 s to 0.009 s in CENA with a most likely value of 0.006 s (6 msec). Hashash et al. (2014) also present computed velocity gradients within the RR layer, $(dV/dz)_{RR}$, ranging from -64 to 46 (m/s)/m with a most likely value of 2 (m/s)/m. This large range of gradients, including negative values, appears to be associated with internal sublayer trends within reference rock as a decrease in velocity gradient is expected with increased depth. Hashash et al. (2014) indicate that within a specific profile, $(dV/dz)$ generally decreases as the profile transitions from weathered rock to reference rock.

Rearranging the terms of Equation 1 and solving for the quality factor leads to the following equation:

$$Q = \frac{H}{V_s \kappa_o} \quad \text{Eq. (4)}$$

The thickness of the reference rock layer was not measured or evaluated by Hashash et al (2014). The following discussion presents three different thicknesses for the RR layer in terms of the quality factor to justify selecting a most likely $H_{RR}$ for the base model. Using the average values for the entire RR layer ($\kappa_o$ = 0.006 s and $V_s$ = 3,250 m/s) and assuming a constant $(dV/dz)_{RR}$ in the RR layer leads to an average quality factor for the RR, $Q_{RR}$, equal to $0.051H_{RR}$. If we consider three possible values for $H_{RR}$: 250, 1,000, and 3,000 m, the corresponding $Q$ values are 13, 51, and 153. These three assumed values of Hrr can also be used to compute the corresponding shear wave velocity gradients using Equation 5: 2, 0.5, and 0.17 (m/s)/s.